

Tumor necrosis factor- α and virus expression in the central nervous system of cats infected with feline immunodeficiency virus

Alessandro Poli^{*1}, Mauro Pistello², Maria Antonietta Carli¹, Francesca Abramo¹, Giulia Mancuso¹, Elisa Nicoletti² and Mauro Bendinelli²

¹Department of Animal Pathology, University of Pisa, Viale delle Piagge, 2, I-56124 Pisa, Italy; ²Retrovirus Center - Department of Biomedicine, University of Pisa, I-56127 Pisa, Italy

Cytokine dysregulation has been implicated in the pathogenesis of lentivirus-induced diseases. In the present study, 18 specific pathogen free (SPF) cats were inoculated with feline immunodeficiency virus (FIV) Petaluma strain and sacrificed at different times post-infection. Five additional SPF cats were used as controls. The cell localization of the cytokine tumor necrosis factor alpha (TNF- α) in the central nervous system (CNS) was determined by immunohistochemical and morphometric analyses with a polyclonal rabbit anti-human TNF- α antibody. TNF- α and FIV RNA were measured using competitive reverse transcriptase polymerase chain reaction (PCR) assays and the number of proviral genomes was estimated by competitive PCR. Portions of frontal cortex were collected from each animal and both formalin-fixed and snap-frozen and stored at -80° C until used. The results showed that TNF- α is present mainly in astrocytes and microglial cells. Morphometric analysis showed that areas of TNF- α production increased in the early phases of infection. Molecular analyses demonstrated that the kinetics of proviral loads in the CNS were comparable to what observed in lymph nodes and peripheral blood mononuclear cells, with the peaks in the early and late stages of infection. A positive correlation was found between viral parameters and TNF- α transcription, the strongest relationship was found between the transcription of the cytokine and viral RNA load. These results confirm that invasion of CNS by FIV occurs soon after virus exposure and that during this phase there is an increase of local viral loads with concomitant up-regulation of TNF- α expression. During the asymptomatic phase viral replication remains low in spite of the progression of CNS alterations. The dissociation between the viral load and the lesions observed suggests the importance of an indirect mechanism for the progression of these lesions, even if TNF- α seems to play a role particularly in the early phase of infection.

Keywords: FIV; central nervous system; TNF- α transcription; proviral load; viral expression; gliosis

Introduction

Central nervous system (CNS) dysfunctions are observed in a large proportion of patients with acquired immunodeficiency syndrome (AIDS), especially in the late stages of the disease (Trillo Pazos and Everall, 1996). Approximately one third of these individuals show severe cognitive and motor deficits known as AIDS dementia (Price *et al*, 1991) or human immunodeficiency virus (HIV)-1 asso-

ciated cognitive/motor complex (Everall *et al*, 1993). The presence of early CNS involvement has been also demonstrated by detection of HIV-1 or its antigens in the cerebrospinal fluid before the onset of neurological symptoms (Gray *et al*, 1996).

The clinical manifestations of AIDS dementia complex result from a diffuse involvement of the CNS characterized by severe pathological abnormalities including HIV meningoencephalitis, neuronal loss, myelin loss and cortical dendritic pathology (Gray *et al*, 1991; Everall *et al*, 1993). Different cells are susceptible to HIV-1 infection in

*Correspondence: A Poli

Received 6 January 1999; revised 8 April 1999; accepted 30 April 1999

the CNS: neurons, astrocytes, macrophages/microglial cells and oligodendroglial cells have been found to be infected by the virus both *in vitro* and *in vivo* (Atwood *et al*, 1993).

The molecular mechanisms responsible for HIV-induced CNS damage remain unclear. Several non-exclusive hypotheses have been proposed including direct toxicity of viral products such as gp 120, immunologically-mediated damage of astrocytes due to the presence of a common epitope on gp 41 and on the astrocytes cell surface antigen, and the production of cytokines such as tumor necrosis factor- α (TNF- α), which impair neuronal function and can cause oligodendroglial cell death and consequent demyelination (Dal Canto, 1997).

Neuropathological changes resembling those observed in HIV-1 infection have been observed in cats infected by feline immunodeficiency virus (FIV), a lentivirus belonging to the same subfamily of HIV and simian immunodeficiency virus (SIV) (Pedersen, 1993; Bendinelli *et al*, 1995). Previous studies by us and others have shown a CNS involvement in FIV-infected cats characterized by perivascular mononuclear cell infiltrates, glial nodules and diffuse gliosis, vacuolar myelinopathy, and meningitis (Dow *et al*, 1990; Hurtrel *et al*, 1992; Podell *et al*, 1993; Poli *et al*, 1997). These changes can be associated with neurological symptoms. CNS involvement in FIV-infected cats, as in HIV-infected persons, is both an early and late event (Hurtrel *et al*, 1992), thus FIV infection of the domestic cat may be a reliable animal model for studying the immunopathogenesis and neuropathological changes that occur in HIV infection.

The purpose of our investigation was to study the viral loads in the frontal cortex of cats at different times post-infection (p.i.) with FIV. To investigate whether TNF- α may be involved in the pathogenesis of neuron damage, transcription of this cytokine and immunocytochemical labeling of TNF- α bearing cells in this portion of the CNS were also analysed using molecular, morphometrical and densitometrical analyses.

Results

At postmortem examination no gross lesions were evident in the brain, spinal cord and meninges of the 18 FIV-infected cats. Confirming previous findings (Poli *et al*, 1997) histopathological examination of selected sections of the frontal cortex revealed moderate to pronounced gliosis involving both gray and white matter and characterized by the presence of swollen astrocytes. Cats sacrificed at 23 months p.i. displayed neuronal alterations characterized by perikarion vacuolization and, in some cases, satellitosis. The results of morphometrical analysis carried out on immunohistochemically stained sections using an anti-gial fibrillary acidic

protein (GFAP) antibody confirmed the presence of generalized astrogliosis (Figure 1A). This was evident as early as 15 days p.i. and, in two of the four subjects examined at this time p.i., GFAP reactivity was markedly higher as compared to the uninfected controls. Astrogliosis was comparably pronounced at 2 months p.i. and was only slightly further increased at 1 year p.i. A more marked

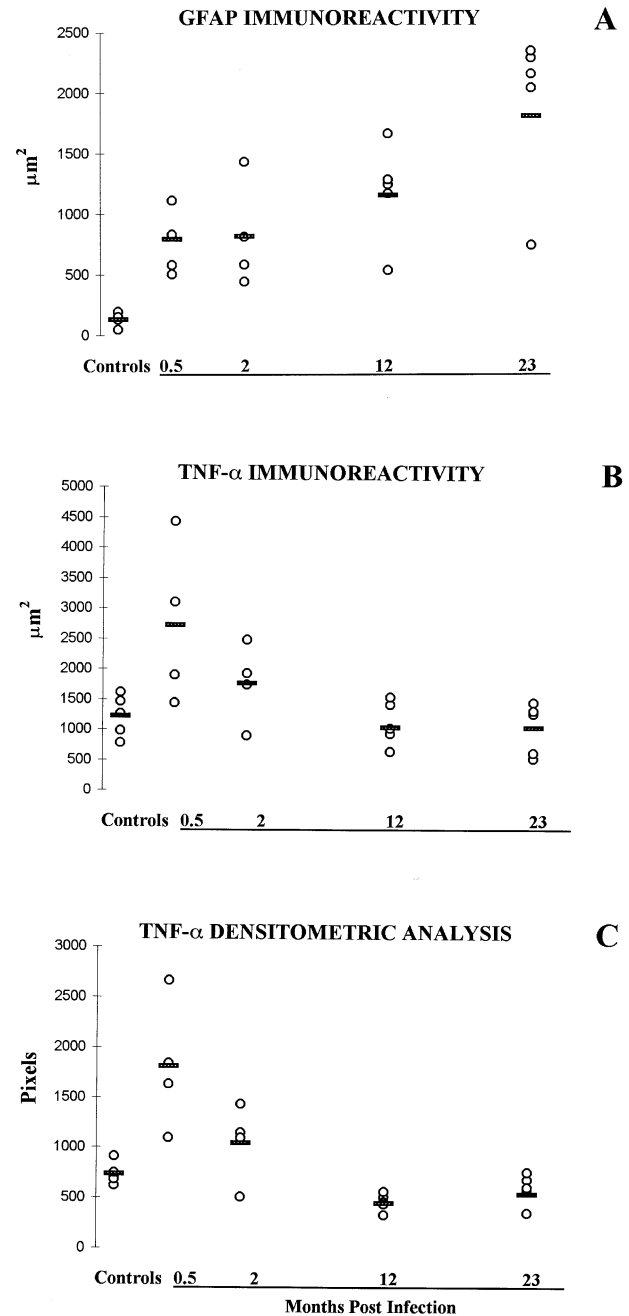


Figure 1 Immunoreactivity for GFAP (A) and TNF- α measured by morphometric (B) or densitometric (C) analysis of the frontal cortex in FIV infected cats sacrificed at different times p.i. and control animals.

increase was seen at 23 months p.i. GFAP reactivity was significantly higher in infected than in control cats ($P=0.0003$). The increase of GFAP reactivity was significantly higher in cats sacrificed at 2 weeks p.i. when compared with controls ($P=0.007$) and in animals examined 23 months p.i. when compared with cats sacrificed at 2 and 12 months p.i. ($P=0.01$). The changes of GFAP reactivity was not significant at the other time points.

Immunohistochemical studies performed to localize the TNF- α protein revealed the presence of scattered immunoreactive cells morphologically similar to astrocytes and microglial cells (Figure 2A). Positive cells were frequently located around blood vessels (Figure 2B). The specificity of the reaction was demonstrated by the lack of immunostaining when the primary antibody was replaced by an unrelated rabbit polyclonal antiserum (Figure 2C).

To better characterize the presence of TNF- α the immunostained sections were submitted to morphometrical and densitometrical studies. Morphometrical analysis revealed an increase of the total area of TNF- α immunoreactivity in three of the subjects examined at 15 days p.i. and in three of four cats sacrificed at 2 months p.i., while the total area of TNF- α immunostaining found in cats at 12 and 23 months p.i. was in the normal range (Figure 1B). Statistical analysis revealed a significant difference in total TNF- α area between infected and control cats ($P=0.02$). Also the mean area of TNF- α immunoreactivity detected in single positive cells was higher at 15 days and 2 months p.i. than at 12 and 23 months p.i. and in the controls (data not shown).

Densitometric analysis confirmed the increase of TNF- α immunoreactivity in the frontal cortex of cats examined at 15 and 2 months p.i. (Figure 1C) ($P=0.0005$). In this early phase, also mean TNF- α immunoreactivity detected in single cells was higher in the infected than in control cats (data not shown).

TNF- α RNA and FIV DNA and RNA in the tissue were measured by quantitative reverse transcriptase (RT)-polymerase chain reaction (PCR) (Figure 3). As expected, there was some variability in the amount of TNF- α transcription detected in individual uninfected cats. On average, however, the levels of TNF- α messenger were higher in infected than in control cats ($P=0.0045$), with peak values detected at 15 days and 2 months p.i. and in one of the longer term infected animals (Figure 4A).

Quantification of FIV DNA showed that the proviral loads in the CNS peaked in the early stages of infection, then subsided to increase again at 23 months p.i. (Figure 4B). The levels of viral RNA followed a similar trend, except that one of the two subjects sacrificed at 15 days p.i. displayed an unexpectedly low RNA burden (Figure 4C). This cat had also a lower viral DNA and RNA content in

PBMC as compared with the mean values found in the other cats at the same time point (1.440 proviral copies/ μ g DNA and 6.650 RNA copies/ μ g RNA versus 3.997 proviral copies/ μ g and 19.177 RNA copies/ μ g RNA, respectively).

In an effort to study the relationships between FIV content and TNF- α production in the CNS, we calculated the regression coefficient between the parameters investigated above. A positive linear

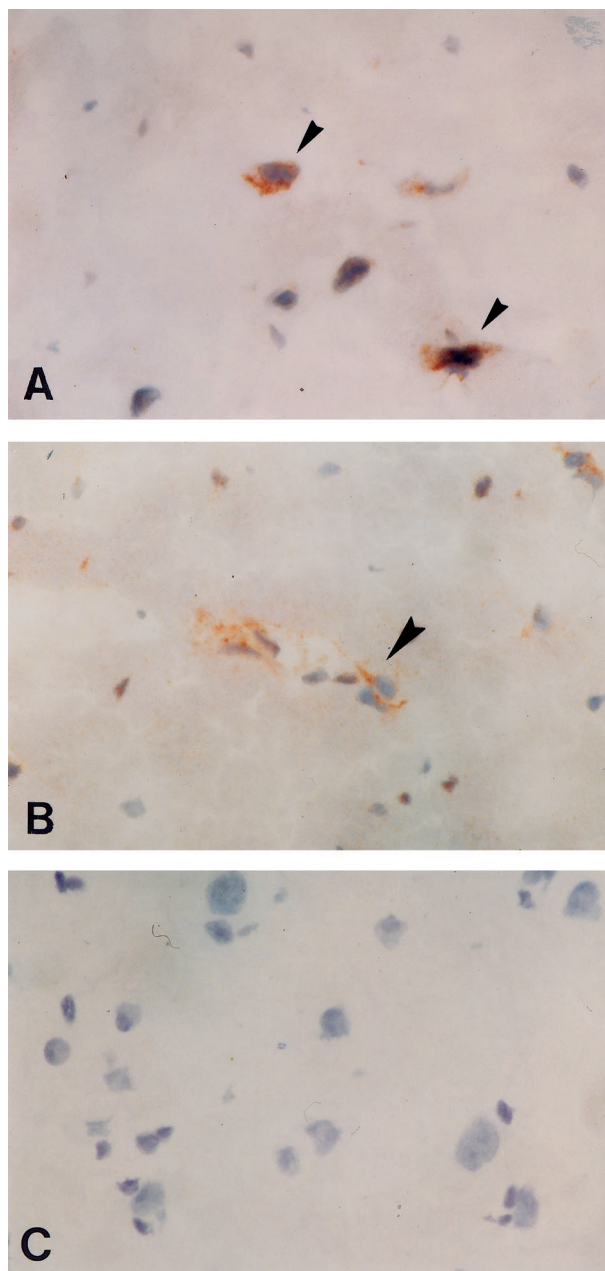


Figure 2 TNF- α immunoreactivity in the gray matter of the frontal cortex of an FIV-infected cat sacrificed 15 days p.i. (A) Scattered TNF- α immunoreactive cells are stained in brown-red (arrows); (B) TNF- α positive cells located around a blood vessel (arrow); (C) lack of immunoreactivity with substitution of primary antiserum with an unrelated rabbit serum.

relationship was found between viral parameters and TNF- α transcription. The strongest relationship was with viral RNA ($r=0.496$, $P=0.0004$), while that with provirus load was lower and had not reached statistical significance. No correlation was instead found between viral DNA and RNA contents and morphometrical and densitometrical data. Also the correlation between TNF- α RNA and TNF- α immunoreactivity did not reach statistical significance. In spite of the lack of correlation the highest levels of TNF- α RNA expression were observed in the subjects with the highest TNF- α immunoreactivity when studied using morphometrical and densitometric analysis.

Discussion

CNS involvement associated with HIV-1 infection is one of the major complications of this disease (An and Scaravilli, 1997). HIV-1 associated neuropathological changes include acute meningoencephalitis, impairment of the blood brain barrier due to vasculitis, vacuolar myelinopathy, and encephalopathy (Budka *et al*, 1991; Gray *et al*, 1996). These changes often cause neurobehavioral changes including cognitive, sensory and motor dysfunctions which may result in profound dementia (Zheng and Gendelman, 1997). The mechanisms by which HIV infection induces these disorders remain unknown for the difficulty of experimental analysis in man because only post-mortem samples and cerebrospinal fluid samples are available. This raised the need for relevant animal models that may help to understand the pathogenesis of HIV-1 associated neuropathology. Among such models FIV is considered suitable to understand the pathogenesis of CNS alterations. In the present study, we have used this model system to investigate in a longitudinal way the relationships between pathological changes, viral loads and TNF- α production in the CNS.

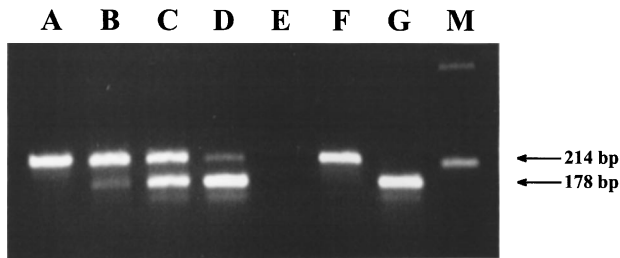


Figure 3 Ethidium bromide stained 2% agarose gel of amplicons obtained from an RT-cPCR used to quantify TNF- α mRNA in the CNS. Lanes A-D, 400 ng CNS RNA/tube plus tenfold dilutions of RNA competitor (from 10^3 to 10^6 copies); lane E no template control; lane F 400 ng CNS RNA alone; lane G: 10^4 copies of RNA competitor alone; M: 100 bp DNA ladder. Positions of amplicons obtained from wild-type (214 bp) and competitor (178 bp) templates are indicated by arrows.

Our results confirm that CNS lesions induced by FIV are similar to those of HIV-1 infection apart from the absence of multinucleated giant cells and are characterized by a slightly increased gliosis in the early phases of infection, and by neuronal damage in later phases (Boche *et al*, 1996; Meeker *et al*, 1997; Poli *et al*, 1997).

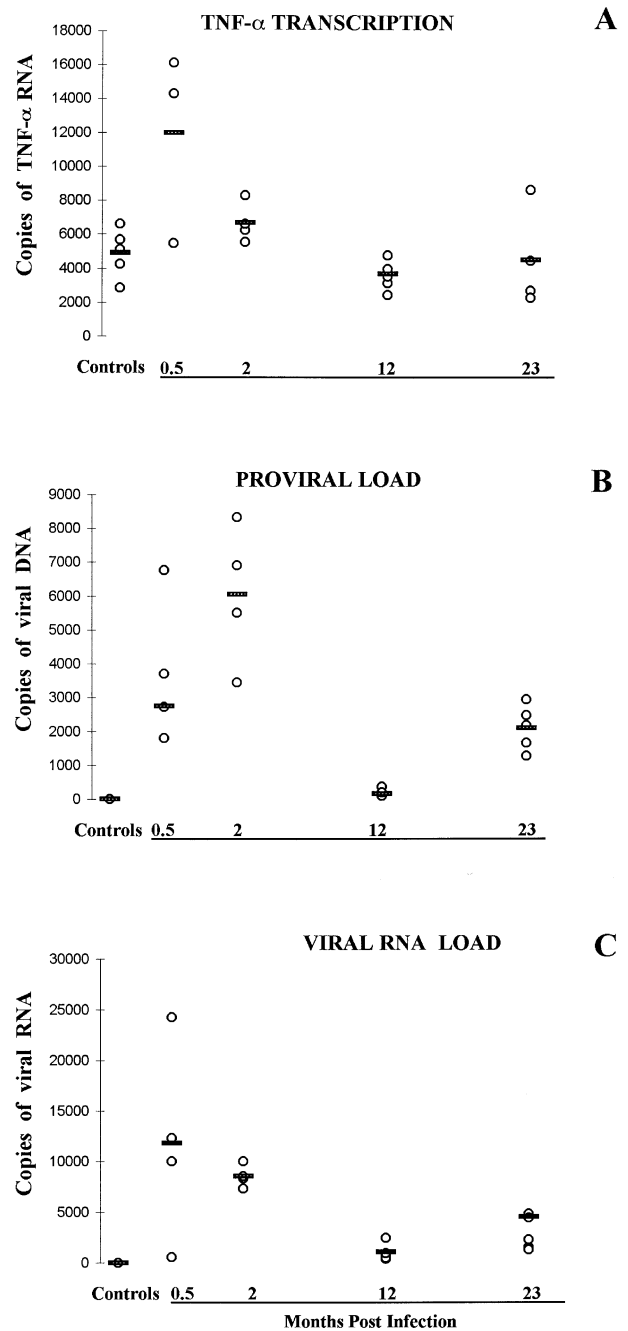


Figure 4 TNF- α transcription (A), proviral DNA (B) and viral RNA genomes (C) in the frontal cortex of FIV infected cats sacrificed at different times p.i. and control animals. The results are expressed as numbers of copies per μ g of tissue RNA (A and C) or DNA (B).

TNF- α , secreted primarily by macrophages, exerts pleiotropic effects on biological and immunological processes (Odeh, 1990) and has been implicated in the pathogenesis of CNS damage by HIV-1 (Atwood *et al*, 1993). This cytokine may be produced by resident cells of the nervous system, specifically astrocytes and microglial cells, or by cells of the immune system that traffic through the CNS (Vilcek and Lee, 1991). TNF- α , together with IL-1 β , has been found to promote astrocytes proliferation (Lachmann *et al*, 1987), a prominent finding observed in FIV and HIV encephalopathy. This cytokine can also cause oligodendroglial death, supporting the hypothesis that TNF- α producing cells may play a role in demyelinating diseases (Robbins *et al*, 1987). TNF- α could also induce expression of MHC class I proteins on astrocytes and oligodendrocytes, exposing these cells to the cytotoxic effects of trafficking cytotoxic T-lymphocytes (Mauerhoff *et al*, 1988). Lastly, TNF- α can upregulate nitric oxide production, which also might represent a means of inducing neuronal injury (Atwood *et al*, 1993).

In this study, we have demonstrated that the recently developed technique based on immunochemical intracellular staining of cytokines (Litton *et al*, 1994) can be used to analyze cytokine-producing cells and study the pathogenesis of lentiviral infections. TNF- α positive cells were detected in sections from both FIV-infected and uninfected cats. The majority of the positively stained cells were recognized on morphological grounds as microglial cells, macrophages around blood vessels or astrocytes. Unfortunately, the lack of antibodies to lineage-specific feline cellular antigens did not allow definitive characterization of TNF- α positive cells.

Transcription and production of TNF- α in astrocytes and microglial cells was significantly up-regulated in the early phase of FIV infection, while these parameters did not change in the animals examined during the asymptomatic phase or later.

As expected, based on previous findings (Beebe *et al*, 1994; Macchi *et al*, 1998), PCR analyses performed for quantitating viral DNA and RNA revealed the highest FIV loads during the early and late stages of infection. Similar to what is observed in the SIV model (Hurtrel *et al*, 1993; Chakrabarti *et al*, 1991), our results confirm that FIV enters the CNS shortly after infection, during initial viremia (Beebe *et al*, 1994; Boche *et al*, 1996). The kinetics of proviral load in the CNS resembled those previously observed by examining lymphoid organs and peripheral blood mononuclear cells (Matteucci *et al*, 1997; Macchi *et al*, 1998), although viral loads in the CNS were consistently lower as compared to what are found in lymphoid tissues.

In the early phases of infection peak TNF- α transcription and production coincided with peaks of viral replication, while at late stage the increased viral burden was accompanied by a moderate

increase of TNF- α transcription only in some cats. In spite of this discrepancy statistical analysis revealed a significant correlation between the extent of viral load and TNF- α transcription. Elevated expression of TNF- α and other cytokine such as interleukin (IL)-1, 4 and 6 has been found in the brain of AIDS patients (An *et al*, 1996; Boche *et al*, 1997). Increased levels of TNF- α mRNA have been also demonstrated in microglial cells and astrocytes of HIV-1-infected patients with clinically evident CNS disfunctions (Nuovo *et al*, 1994). Envelope glycoprotein 120 (gp 120) seems to play a role in this cytokine dysregulation which may participate in the initiation and propagation of HIV-1 neuropathology. In fact, an increased expression of mRNAs of proinflammatory cytokines such as IL-1 β , TNF- α , and TGF- β has been induced in the hypothalamus of Wistar rats in response to the chronic intracerebroventricular microinfusion of HIV-1 derived gp 120 (Ilyin and Plata Salamàn, 1997).

The dissociation between the low viral load observed during the asymptomatic phase of the infection and the progression of CNS alteration revealed in FIV-infected cats in our previous study (Boche *et al*, 1997) supports the importance of an indirect mechanism for the pathogenesis of neuropathological alterations detected in these subjects. Furthermore the severe lesions and neurological dysfunctions described in HIV-1 and FIV infections (Lafrado *et al*, 1993; Phillips *et al*, 1994, 1996) do not appear to be justified by the low number of virus-producing cells detected locally (Nuovo *et al*, 1994; Boche *et al*, 1996; Poli *et al*, 1997).

In conclusion, our findings suggest that TNF- α production is activated in the CNS parenchyma of FIV-infected cats in the early phase of the infection. These results support the hypothesis that neurotoxic factors released from non-neuronal cells such as astrocytes, microglial cells or macrophages may participate in the pathogenesis of the brain damage observed in lentiviral infections.

Materials and methods

Animals

Eighteen specific pathogen free (SPF) female cats, between 1 and 4 years of age, were used in the study. The subjects were infected with the Petaluma strain of FIV by inoculation of culture supernatant of persistently infected FL4 cells (Yamamoto *et al*, 1991) containing approximately 20–50% cat infectious doses. Five FIV-seronegative SPF cats were used as controls. Infected and control cats were housed in isolation units (Techniplast, Gazzada, Italy) at the Retrovirus Center of the University of Pisa and examined daily throughout the observation period. Physical examination, including measurements of body weight and clinical neurological investigations, were performed weekly for the first 2

months p.i. and then monthly. Neurological examination consisted of overall assessment of the animals' mental state, behavior, gait, posture and movement. The presence of specific anti-FIV antibodies was determined using an in-house enzyme linked immunosorbent assay (Lombardi *et al*, 1994) and was confirmed by Western blot analysis on electrophoresed FIV proteins from gradient-purified tissue culture grown virus. All infected cats seroconverted at 4–6 weeks p.i. and exhibited a progressive reduction in the number of circulating CD4⁺ T-lymphocytes, that in several cats declined by almost two-thirds over the course of 1 year. Groups of animals were induced to deep anaesthesia and necropsied at 0.5 (four cats), 2 (four cats), 12 (five cats) and 23 (five cats) months p.i. At the time of sacrifice, none of the cats exhibited obvious neurological signs.

Tissue processing

Brains were obtained immediately after necropsy. Samples of frontal cortex were fixed in 10% buffered formalin (pH 7.4), embedded in paraffin, and stained by routine neuropathological stains. Sections were stained with Gram, Ziehl-Nielsen, periodic acid Schiff, and Grocott stains in order to exclude opportunistic infections. Paraffin sections were stained with polyclonal antiserum directed to GFAP (Biogenex Lab, San Ramon, CA, USA) in a Shandom Sequenza immunostaining method as previously described (Abramo *et al*, 1995) for the identification of astrocytes.

Samples were also stored at -80°C for molecular analysis and localization of TNF- α by immunocytochemistry. TNF- α reactivity was determined on formalin fixed and frozen sections by using a polyclonal rabbit anti-human TNF- α antiserum (BioSource International, Camarillo, CA, USA), and detection was by a peroxidase biotin-streptavidin system (Biogenex). Briefly, after incubation with the primary antiserum for 1 h at room temperature in a moist chamber, sections were extensively washed and then incubated with a biotinylated affinity purified goat anti-rabbit secondary antibody (Biogenex) for 30 min. Sections were again washed before incubation for 1 h in a streptavidin-horse-radish peroxidase complex (Biogenex) and the reaction was developed in an aminoethylcarbazole substrate for 10 min.

Morphometric analysis

GFAP and TNF- α reactivity were measured using a semiautomatic computer analysis system. Ten microscopic fields ($25\times$ objective) were captured by a television camera and projected onto the monitor screen of a semiautomatic image analysis system (Quantimet 500 MC, Leica). The areas of GFAP reactive astrocytes and TNF- α positive cells were measured and total area per micro-

scopic field ($235\ \mu\text{m}^2$) was calculated and given in square microns (μm^2).

Densitometric analysis

The sections underwent densitometric analysis of TNF- α positive cells by using the above video-based computer-linked system programmed to stain the immunoreactive substances in gray. Briefly, the densitometer was calibrated daily to ensure constant conditions throughout the experiment, the light setting was constant for each measuring series, and the images were taken through a $\times 40$ objective with a black and white television camera and transferred to the screen. The microscopic field analyzed was $145\ \mu\text{m}^2$. The instrument was initially calibrated in the gray level analysis mode (256 gray levels) by determining the gray level (density) of a predetermined clear (gray=256) and dark (gray=1) region of a standard section. The number of pixels activated by the label in each structure was read and calculated by the computer microdensitometer. Threshold values for the detection of the label were fixed for each field so that the computer would read only the label present in the selected structures. For each section, the number of labeled structures (TNF- α reactive cells), the total area of immunoreactive substance and the number of pixels per gray level were measured. Subsequently, the sum of the product of number of pixels corresponding to the gray levels (this sum represents a relative quantitative evaluation of the antigen content) and the immunoreactivity per unit area was calculated.

Molecular analyses

Genomic DNA was extracted from frozen sections of the frontal cortex as described (Macchi *et al*, 1998). RNA was extracted from 100–500 mg tissue by using a guanidinium-isothiocyanate acidic phenol method (Gene Dia, Lammari, Lucca, Italy) in PCR-clean conditions, pelleted, and resuspended in $40\ \mu\text{l}$ nuclease-free water.

FIV DNA and RNA sequences were detected by *gag*-specific nested- and RT-nested PCR, respectively. Positive samples were subsequently analyzed with competitive-PCR (cPCR) and RT-cPCR with a deleted internal control which permitted FIV DNA and RNA quantitations (Pistello *et al*, 1994, 1997, 1999).

Transcription of fTNF- α was measured by RT-cPCR with a deleted internal control and a primer set (TNF-F: 192-CCC ACA TGG CCT GCA ACT AAT-212; TNF-R 406-AGA TGA GGT ACA GCC CGT CTG A-385, nucleotide position referred to fTNF- α mRNA, Gene Bank accession number M92061) deduced from the second (TNF-F) and the fourth (TNF-R) exons of fTNF- α gene (Gene-Bank accession numbers: X54000 and M92061), to be able to distinguish RNA-derived from DNA-derived PCR products. The thermocycling profile of RT-PCR was the

following: RT: 42°C 1 h, 95°C 5 min; amplification: 94°C 2 min, denaturation 94°C 20 s, 55°C 15 s, 72°C 30 s for 50 cycles, followed by a final incubation at 72°C for 10 min.

The deleted internal control was produced from a TNF- α amplified product that was diluted and reamplified using the TNF-R primer and a modified TNF-F (primer TNF-FD: 192-CCC ACA TGG CCT GCA ACT AAT AAC TCC GAG TGA CAA GCC AGT-269). This oligonucleotide covers the same position of TNF-F, but is longer and lacks the nucleotides from 212–248 bp. Thus, amplification of full-length amplicon (214 bp) with TNF-FD and TNF-R produces a 36 bp-deleted fragment (178 bp). The thermocycling conditions, conducted for 25 cycles, were identical to those for the amplification described above. The deleted fragment was subsequently diluted and amplified using tailed primers TNF-F and TNF-R bearing promoter sequences for the T7 RNA-polymerase and the SP6 RNA-polymerase, respectively. Optimal thermocycling conditions had been established to be: 94°C 2 min, 5 cycles at 94°C 30 s, 55°C 30 s, and 72°C 1 min; 25 cycles at 94°C 30 s, 65°C 30 s, and 72°C 1 min; final extension 72°C 10 min. Sense RNA templates were then produced from 300 ng of this amplified product by using an *in vitro* run-off transcription and the Riboprobe Combination System SP6/T7 RNA polymerase kit (Promega, Madison, WI, USA). Transcripts were purified from the DNA template by digestion with RNase-free DNase (1 U/ μ g of DNA) for 1 h at 37°C and then at 70°C for 15 min to inactivate the DNase. Finally, RNA was purified by phenol-chloroform extraction and alcohol precipitation, suspended in nuclease-free water, quantitated by OD at 260 nm, and analyzed on a 10% polyacrylamide gel to check for its integrity and absence of DNA

References

Abramo F, Bo S, Canese MG, Poli A (1995). Regional distribution of lesions in the central nervous system of cats infected with feline immunodeficiency virus. *AIDS Res Hum Retroviruses* **11**: 1247–1253.

An SF, Scaravilli F (1997). Early HIV-1 infection of the central nervous system. *Arch Anat Cytol Pathol* **45**: 94–105.

An SF, Ciardi A, Giometto B, Scaravilli T, Gray F, Scaravilli F (1996). Investigation on the expression of major histocompatibility complex class II and cytokines and detection of HIV-1 DNA within brains of asymptomatic and symptomatic HIV-1 positive patients. *Acta Neuropathol* (Berl) **91**: 494–503.

Atwood WJ, Berger JR, Kadermann R, Tornatore CS, Major EO (1993). Human immunodeficiency virus type 1 infection of the brain. *Clin Microbiol Rev* **6**: 339–366.

template. RNA transcripts were diluted in tenfold steps from 10^7 to 10^2 RNA copies/5 ml and stored at -80°C until used.

Competitive RT-PCR for TNF- α RNA was carried out by adding 50 ng of tissue RNA and 5 ml of competitor RNA dilutions to 10 ml of an RT-mixture containing 40 pmol TNF-R and 6 U avian myeloblastosis virus RT (Promega, Madison, WI, USA). Reactions were incubated at 42°C for 1 h followed by RT inactivation at 95°C for 5 min. PCR was performed by adding to each well a master mix (80 μ l) containing 40 pmol TNF-F and 1 U *Taq* DNA polymerase (Perkin Elmer, Foster, CA, USA). The amplification profile used was the same as described above. Analysis and quantitation of PCR products were carried out as for quantitative PCR (Pistello *et al*, 1994). The point at which sample RNA gave a signal equivalent to the competitor was used to calculate the RNA equivalents per μ g tissue RNA. The method consistently detected as few as 100 copies of the RNA competitor.

Statistical analysis

Normal distribution was tested with the Kolmogorov-Smirnov test. Group means \pm s.d. were calculated. Analysis of variance was carried out and significance of differences between groups was evaluated with one way Anova and linear fit. Mean values of GFAP reactivity observed in cats sacrificed at different time points were compared using an independent-samples *t*-test (IMPr Statistic modal visual 3.1, SAS Institute Inc., Cary, NC, USA).

Acknowledgements

This study was supported by a grant from Ministero della Sanità-Istituto Superiore di Sanità Programma per l'AIDS, Rome (Italy).

Beebe AM, Dua N, Faith TG, Moore PF, Pedersen NC, Dandekar S (1994). Primary stage of feline immunodeficiency virus infection: viral dissemination and cellular targets. *J Virol* **68**: 3080–3091.

Bendinelli M, Pistello M, Lombardi S, Poli A, Matteucci D, Ceccherini-Nelli L, Malvaldi G, Tozzini F (1995). Feline immunodeficiency virus: an interesting model for AIDS studies and an important cat pathogen. *Clin Microbiol Rev* **8**: 87–112.

Boche D, Hurtrel M, Gray F, Claossens-Maire M-A, Ganière J-P, Motagnier L, Hurtrel B (1996). Virus load and neuropathology in the FIV model. *J Neurovirol* **2**: 377–387.

Boche D, Gray F, Khatissian E, Hurtrel M, Montagnier L, Hurtrel B (1997). Contribution of animal models in the understanding of AIDS encephalopathy. *Arch Anat Cytol Pathol* **45**: 75–85.

- Budka H, Wiley CA, Kleihues P (1991). HIV-associated disease of the nervous system: review of nomenclature and proposal for neuropathology based terminology (consensus report). *Brain Pathol* **1**: 143–152.
- Chakrabarti L, Hurtrel M, Maire M-A, Vazeux R, Dormont DD, Montagnier L, Hurtrel B (1991). Early viral replication in the brain of SIV-infected rhesus monkeys. *Am J Pathol* **139**: 1273–1280.
- Dal Canto MC (1997). Mechanisms of HIV infection of the central nervous system and pathogenesis of AIDS-dementia complex. *Neuroimaging Clin N Am* **7**: 231–241.
- Dow SW, Poss ML, Hoover EA (1990). Feline immunodeficiency virus: A neurotropic lentivirus. *J Acquir Immune Defic Syndr* **3**: 658–668.
- Everall I, Luthert P, Lantos P (1993). A review of neuronal damage in human immunodeficiency virus infection: Its assessment, possible mechanism and relationship to dementia. *J Neuropathol Exp Neurol* **52**: 561–566.
- Gray F, Geny C, Lionnet F, Dournon E, Fénelon G, Gherardi R, Poirier J (1991). Etude neuropathologique de 135 cas adultes de syndrome d'immunodéficience acquise (SIDA). *Ann Pathol* **11**: 236–247.
- Gray F, Scaravilli F, Everall I, Chretien F, An S, Boche D, Adle Biassette H, Wingertsmann L, Durigon M, Hurtrel B, Chiodi F, Bell J, Lantos P (1996). Neuropathology of early HIV-1 infection. *Brain Pathol* **6**: 1–15.
- Hurtrel M, Ganière JP, Guelfi JF, Chakrabarti L, Maire M-A, Gray F, Montagnier L, Hurtrel B (1992). Comparison of early and late feline immunodeficiency virus encephalopathies. *AIDS* **6**: 399–406.
- Hurtrel B, Chakrabarti L, Hurtrel M, Montagnier L (1993). Target cells during early SIV encephalopathy. *Res Virol* **144**: 45–49.
- Ilyin SE, Plata Salamàn CR (1997). HIV-1 gp 120 modulates hypothalamic cytokine mRNAs in vivo: implications to cytokine feedback systems. *Biochem Biophys Res Commun* **231**: 514–518.
- Lachman LB, Brown DC, Dinarello CA (1987). Growth-promoting effect of recombinant interleukin 1 and tumor necrosis factor for a human astrocytoma cell line. *J Immunol* **138**: 2913–2916.
- Lafrado L, Podell M, Krakowa S, Hayes K, Hanlen M, Mathes L (1993). FIV: a model for retrovirus-induced pathogenesis. *AIDS Res Review* **3**: 115–150.
- Litton MJ, Sauder B, Murphy E, O'Garra A, Abrams JS (1994). Early expression of cytokine in lymph nodes after treatment *in vivo* with Staphylococcus enterotoxin B. *J Immunol Methods* **175**: 47–58.
- Lombardi S, Poli A, Massi C, Abramo F, Zaccaro L, Bazzichi A, Malvaldi G, Bendinelli M, Garzelli C (1994). Detection of feline immunodeficiency virus p24 and p24-specific antibodies by monoclonal antibody-based assays. *J Virol Methods* **46**: 287–301.
- Macchi S, Maggi F, Di Iorio C, Poli A, Bendinelli M, Pistello M (1998). Detection of feline immunodeficiency proviral sequences in lymphoid tissues and central nervous system by *in situ* gene amplification. *J Virol Methods* **73**: 109–119.
- Matteucci D, Pistello M, Mazzetti P, Giannecchini S, Del Mauro D, Lonetti I, Zaccaro L, Pollera C, Specter S, Bendinelli M (1997). Studies on AIDS vaccination using an *ex vivo* feline immunodeficiency virus model: protection conferred by a fixed cell vaccine against cell-free and cell-associated challenge differs in duration and is not easily boosted. *J Virol* **71**: 8368–8376.
- Mauerhoff T, Pujol-Borrell R, Mirakian R, Bottazzo GF (1988). Differential expression and regulation of major histocompatibility complex (MHC) products in neural and glial cells of the human fetal brain. *J Neuroimmunol* **18**: 271–289.
- Meeker RB, Thiede BA, Hall C, English R, Tompkins M (1997). Cortical cell loss in asymptomatic cats experimentally infected with feline immunodeficiency virus. *AIDS Res Human Retroviruses* **13**: 1131–1140.
- Nuovo GJ, Gallery F, MacConnell P, Braun A (1994). *In situ* detection of polymerase chain reaction-amplified HIV-1 nucleic acids and tumour necrosis factor- α RNA in the central nervous system. *Am J Pathol* **144**: 659–666.
- Odeh M (1990). The role of tumour necrosis factor- α in acquired immunodeficiency syndrome. *J Int Med* **228**: 549–556.
- Pedersen NC (1993). Feline immunodeficiency virus infection. In: *The Retroviruses*, Vol 2, Levy JA (Ed). Plenum Press, New York, pp 181–228.
- Phillips TR, Prospero-Garcia O, Puaoli DL, Lerner DL, Fox HS, Olmsted RE, Bloom FE, Henriksen SJ, Elder JH (1994). Neurological abnormalities associated with feline immunodeficiency virus infection. *J Gen Virol* **75**: 979–987.
- Phillips TR, Prospero-Garcia O, Wheeler DW, Wagaman PC, Lerner DL, Fox HS, Whalen LR, Bloom FE, Elder JH, Henriksen SJ (1996). Neurologic dysfunction caused by a molecular clone of feline immunodeficiency virus. *J Neurovirol* **2**: 388–396.
- Pistello M, Menzo S, Giorgi M, Da Prato L, Cammarota G, Clementi M, Bendinelli M (1994). Competitive polymerase chain reaction for quantitating feline immunodeficiency virus load in infected cat tissues. *Mol Cell Probes* **8**: 229–234.
- Pistello M, Cammarota G, Nicoletti E, Matteucci D, Curcio M, Del Mauro D, Bendinelli M (1997). Analysis of the genetic diversity and phylogenetic relationship of Italian isolates of feline immunodeficiency virus indicates high prevalence and heterogeneity of subtype B. *J Gen Virol* **78**: 2247–2257.
- Pistello M, Matteucci D, Cammarota G, Mazzetti P, Giannecchini S, Del Mauro D, Macchi S, Zaccaro L, Bendinelli M (1999). Kinetics of preinfecting and challenge virus replication during a three year interclade feline immunodeficiency virus superinfection experiment in cats. *J Virol* **73**: 1518–1527.
- Podell M, Oglesbee M, Mathes L, Krakowka S, Olmstead R, Lafrado L (1993). AIDS-associated encephalopathy with experimental feline immunodeficiency virus infection. *J Acquir Immune Defic Syndr* **6**: 758–771.



- Poli A, Abramo F, Di Iorio C, Cantile C, Carli MA, Pollera C, Vago L, Tosoni A, Costanzi G (1997). Neuropathology in cats experimentally infected with feline immunodeficiency virus: a morphological, immunocytochemical and morphometric study. *J Neurovirol* **3**: 361–368.
- Price RW, Sidtis JJ, Brew BJ (1991). AIDS dementia complex and HIV-1 infection: a view from the clinic. *Brain Pathol* **1**: 155–162.
- Robbins DS, Shirazi Y, Drysdale B, Lieberman A, Shin HS, Shin ML (1987). Production of cytotoxic factor for oligodendrocytes by stimulated astrocytes. *J Immunol* **139**: 2593–2597.
- Trillo Pazos G, Everall IP (1996). Neuronal damage and its relation to dementia in acquired immunodeficiency syndrome (AIDS). *Pathobiology* **64**: 295–307.
- Vilcek J, Lee TH (1991). Tumor necrosis factor. New insights into the molecular mechanisms of its multiple actions. *J Biol Chem* **266**: 7313.
- Yamamoto JK, Ackley CD, Zochlinski H, Louie H, Pembroke E, Torten M, Hansen H, Munn R, Okuda T (1991). Development of IL-2-independent feline lymphoid cell lines chronically infected with feline immunodeficiency virus: Importance for diagnostic reagents and vaccines. *Intervirology* **32**: 361–375.
- Zheng J, Gendelman HE (1997). The HIV-1 associated dementia complex: a metabolic encephalopathy fueled by viral replication in mononuclear phagocytes. *Curr Opin Neurol* **10**: 319–325.